Physical encapsulation of droplet interface bilayers for durable, portable biomolecular networks

Stephen A. Sarles[a] and Donald J. Leo*[b]

Received 14th August 2009, Accepted 19th November 2009
First published as an Advance Article on the web 6th January 2010
DOI: 10.1039/b916736f

Physically-encapsulated droplet interface bilayers are formed by confining aqueous droplets encased in lipid monolayers within connected compartments of a solid substrate. Each droplet resides within an individual compartment and is positioned on a fixed electrode built into the solid substrate. Full encapsulation of the network is achieved with a solid cap that inserts into the substrate to form a closed volume. Encapsulated networks provide increased portability over unencapsulated networks by limiting droplet movement and through the integration of fixed electrodes into the supporting fixture. The formation of encapsulated droplet interface bilayers constructed from diphytanoyl phosphocoline (DPhPC) phospholipids is confirmed with electrical impedance spectroscopy, and cyclic voltammetry is used to measure the effect of alamethicin channels incorporated into the resulting lipid bilayers. The durability of the networks is quantified using a mechanical shaker to oscillate the bilayer in a direction transverse to the plane of the membrane and the results show that single droplet interface bilayers can withstand 1–10*g* of acceleration prior to bilayer failure. Observed failure modes include both droplet separation and bilayer rupturing, where the geometry of the supporting substrate and the presence of integrated electrodes are key contributors. Physically-encapsulated DIBs can be shaken, moved, and inverted without bilayer failure, enabling the creation of a new class of lab-on-chip devices.

Introduction

The droplet interface bilayer (DIB) forms the basis for a new class of material system that utilizes the functions of biomolecules for converting energy, sending and receiving information, catalyzing reactions, and providing selective transport of species. In its original form,[1–4] DIB networks consist of lipid-encased water droplets that are connected to form aqueous networks submerged in an organic solvent. The interface that physically connects adjacent droplets in these networks is a lipid bilayer that is capable of supporting functional biomolecules, such as proteins, which self-assemble directly from the internal volumes of the neighboring droplets into the interfacial bilayer. This technique highlights (and relies on) the self-assembly processes of both the phospholipid molecules that form lipid monolayers at the oil/water interface surrounding the droplets and the proteins that self-insert into the interfacial bilayers.

Previous research has demonstrated that this method can be used to create durable networks of lipid bilayers where the arrangement and contents of the droplets determine the functionality of the network.[2,3,5] In their initial paper, Holden *et al.* harvested light-energy using bacteriorhodopsin proteins contained in satellite droplets that when irradiated with light produced proton currents which were channeled into a central droplet. The same group recently used genetically-modified alpha-hemolysin channels to coordinate diode-like current rectification of specific interfaces for collective processing in multi-droplet bridge rectifier circuits.[6] Parallel research by our group has also shown that external feedback control, in addition to biomolecules incorporated within the lipid interfaces, can be used to tailor the current–voltage properties of droplet interface bilayers.[7] Through droplet composition, network arrangement, and electrical stimulation the DIB method offers great versatility for constructing useful biomolecular assemblies pertinent to the development of novel drug delivery systems,[8] high-throughput screening,[9,10] and *in vitro* compartmentalization of cellular components for studying the link between genotype and phenotype.[11]

Transitioning this technology into packaged lab-on-chip device concepts, though, is hindered by the limited portability of the original embodiment of a DIB network. The results presented in this paper initiate the design and development of a solid supporting substrate that physically encapsulates biomolecular networks formed from droplet interface bilayers. A prototype substrate made from acrylic (PMMA) that features integrated electrodes is fabricated and characterized for encapsulating DIBs. The initial results demonstrate that through physical encapsulation, these networks can be moved, shaken, and even inverted while retaining functioning lipid bilayer interfaces. We also present data on the quantification of DIB durability under mechanical vibration, both for unencapsulated DIBs and physically-encapsulated networks.

Encapsulation methodology and definitions

We denote the original form of the droplet-interface bilayer as the *liquid-in-liquid* form due to the fact that the lipid-encased aqueous droplets are surrounded by a large volume of organic

[a]*Department of Mechanical Engineering, Virginia Tech, Blacksburg, VA, USA*
[b]*Department of Mechanical Engineering, Virginia Tech, Blacksburg, VA, USA. E-mail: donleo@vt.edu*

solvent (Fig. 1a). As demonstrated by Holden *et al.*, the liquid-in-liquid form enables easy reconfiguration of multi-droplet networks by rearrangement of individual droplets.[2,4]

While the liquid-in-liquid form of the DIBs has advantages in reconfigurability, modifications are required for applications that necessitate durable and portable DIB networks. The liquid-in-liquid form does not prevent large motion of the droplets when the substrate is moved and, in our work, it is often the case that droplet coalescence due to bilayer failure occurs when the substrate is moved. Furthermore, simple actions such as inverting the network are not possible using the original liquid-in-liquid form of DIB networks. While the liquid-in-liquid form is useful for many applications, such as controlled laboratory environments, our goal in this paper is to demonstrate that more-portable and durable devices are possible with DIB networks formed in new substrates.

In our work we have focused on developing droplet-interface bilayer networks that are encased in a solid substrate to increase network portability and durability. Our method is based on the placement of lipid-encased droplets into substrates that have compartments that are sized to hold single droplets surrounded by a small volume of organic solvent (shown in Fig. 1b). One of the key aspects of this approach is that the droplets are restrained from large motions by the surrounding solid substrate. For this reason, we denote any substrate that restrains large motions of the droplet as *encapsulation*. Furthermore, the methodology that we study in this paper is termed *physical encapsulation* of the droplets to differentiate it from other means of restraining droplet motion, such as polymerization of the surrounding organic solvent that results in chemical encapsulation of the droplets. For the remainder of this paper, we will refer to the liquid-in-liquid form of the DIBs as *unencapsulated* to highlight the fact that the surrounding substrate does not restrain large motion of the droplets.

Also in this paper we define a parameter called the packing factor to quantify the differences in the unencapsulated and encapsulated substrates. The packing factor is defined as the ratio of the droplet volume to the total volume of the droplet and organic solvent. In this paper we study two packing factors that are significantly different to ascertain the key aspects of unencapsulated and encapsulated substrates. A *low packing factor*, on the order of 1%, is shown for the substrate illustrated in Fig. 1a. This substrate has properties that are similar to those studied by Holden *et al*, in their original work and require the use of suspended electrodes for probing the network.[2,7,12] Droplets are placed in small divots in the solid substrate and surrounded by a large volume of organic solvent.

A two-droplet high-packing factor substrate introduced in this paper and shown in Fig. 1b consists of two wells drilled into a solid PMMA substrate. The bottom of each compartment is rounded to mimic the divots that are placed in the low-packing factor substrate. The packing factor for a 350 nl droplet (875 μm in diameter) residing in each droplet compartment in this substrate is approximately 32%, when only the total volume of the droplet compartments is considered. It is estimated that a 50–75 μm layer of hexadecane resides between each droplet and the surrounding acrylic substrate as measured along the droplet perimeter. For this work a packing factor of >30% is denoted "high", and we have fabricated substrates that have packing factors on the order of 50–60% depending on the depth of the wells and the size of the droplets.

The remainder of this work is focused on demonstrating that encapsulated DIB networks with integrated electrodes can be formed in solid substrates. The properties of two- and three-droplet networks are quantified in a series of electrical and mechanical tests, and the results are compared to baseline results on an unencapsulated two-droplet network to demonstrate that encapsulated networks retain all the critical properties of unencapsulated networks.

Results and discussion

Baseline characterization of unencapsulated DIBs

For comparison purposes, unencapsulated droplet interface bilayers composed of diphytanoyl phosphocholine (DPhPC) phospholipids are formed in a low-packing factor substrate (Fig. 1a) where suspended, wire-type silver–silver chloride (Ag/AgCl) electrodes are used for droplet positioning and electrical interrogation.[2,7] Electrical impedance spectroscopy (EIS) measurements verify the formation of a bilayer at the interface of neighboring droplets and cyclic voltammetry (CV) measurements confirm the incorporation of alamethicin channels into the resulting interfacial bilayer (Fig. 2, a and b). EIS

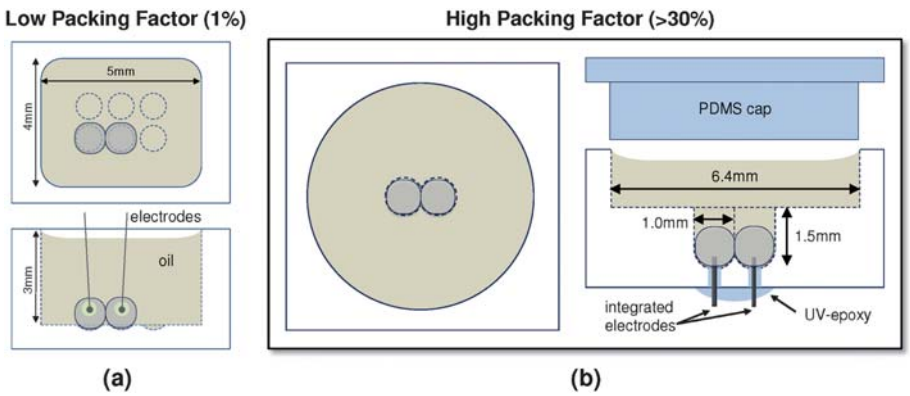

Fig. 1 Unencapsulated DIBs are formed in a low packing factor substrate (a), while physically-encapsulated droplet interface bilayers are formed in a new high packing factor substrate that confines aqueous droplets submerged in oil to specific positions and features integrated electrodes for electrical interrogation (b).

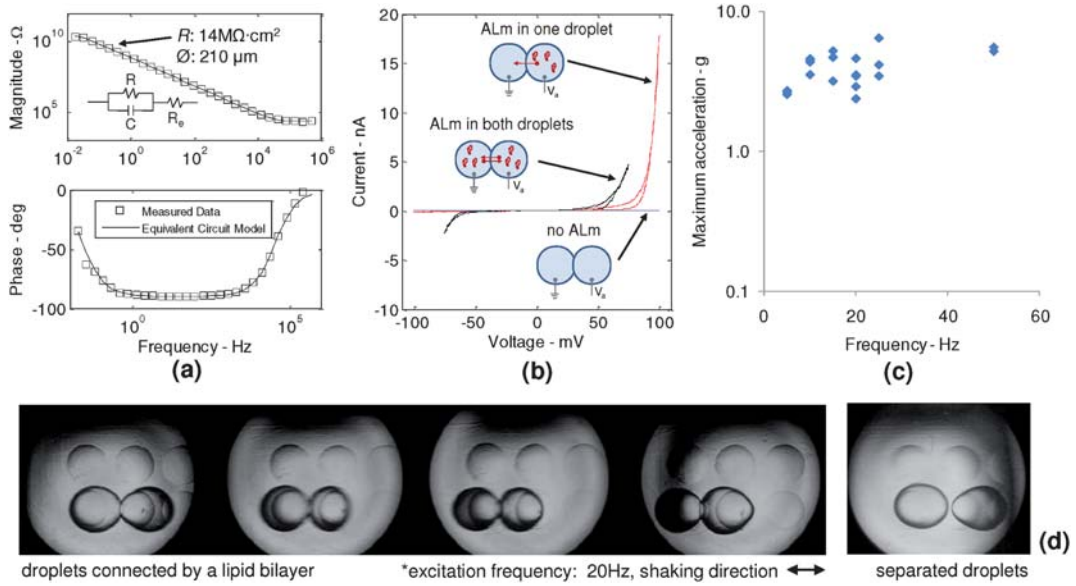

Fig. 2 Unencapsulated DIBs are characterized with both electrical and mechanical tests. EIS (a) and CV (b) measurements on these droplet pairs verify and quantify the formation of a bilayer at the interface of two adjacent droplets and show how proteins incorporated into the droplets can be used to tailor the current–voltage relationship of an interface, respectively. The measured accelerations that cause complete bilayer unzipping (c) provides quantification of the observed durability of unencapsulated DIBs (d).

measures the resistance to charge transport across the droplet interface positioned between the electrodes within neighboring droplets. When no bilayer forms (and the droplets remain separate), EIS measurements indicate an "open circuit" response. When the droplets coalesce, the measurement records the impedance of the lipid–electrolyte solution. Conversely, measurements of a lipid bilayer are characterized by a high electrical impedance magnitude (>1 GΩ) and a phase angle approaching 0° (*i.e.* resistive behavior) at frequencies less than 1 Hz and by a decreasing magnitude of impedance corresponding to a phase angle of −90° (*i.e.* capacitive behavior) at frequencies between 1 Hz–10 kHz (Fig. 2a). The high-frequency asymptote of the magnitude (10 kΩ) and phase (0°) for the impedance of a droplet interface bilayer corresponds to the resistance of the electrolyte present within each droplet. The experimental data is fitted with an equivalent electrical circuit (shown in Fig. 2a) in order to obtain estimates of the resistance and capacitance of the lipid bilayer.[13,14] Estimates of bilayer capacitance obtained from EIS data agree well with those values reported for bilayer interfaces formed between droplets of similar size.[2] Typical droplet interface bilayers formed between 350 nl droplets have nominal values of bilayer resistance greater than 10 GΩ and equivalent diameters of the interface of 200–400 μm (using a specific capacitance for DPhPC bilayers of 0.6 μF/cm^2 [15]). Alamethicin channel activity is witnessed in the cyclic voltammetry measurements; namely the direction of insertion of these channels produces either asymmetric or symmetric current–voltage relationships when only one droplet contains alamethicin or when both droplets contain the protein. Alamethicin is a 2 kDa ion channel that binds to and partially inserts into a bilayer as a monomer and then upon application of voltage, inserts through the hydrophobic core of the membrane and aggregates with other monomers to form cation-selective ion channels.[16–18]

We have observed that unencapsulated droplet interface bilayers undergo large movements when the surrounding substrate is handled or shaken which can result in droplet separation. Mechanical testing of two-droplet unencapsulated networks (without suspended electrodes) consistently shows that large deformations of the droplets under lateral acceleration in the direction perpendicular to the plane of the membrane cause the droplets to separate (Fig. 2d). We believe that these deformations, in addition to the resulting forces on the interface due to out-of-phase motions of the two droplets, result in the creation of new oil/water interface that effectively raises the surface tension of each droplet and which acts to unzip the bilayer at the interface. Additionally, image processing of the movements of the droplet pairs during shaking permits the estimation of the droplet pair acceleration relative to the motion of the substrate for quantitatively characterizing DIB durability. The connected droplet pairs exhibit amplified motions (3–5×) relative to the dynamics of the supporting substrate at frequencies near 20 Hz, with amplification ratios diminishing to a value of 1 for excitation frequencies near 20 Hz and amplification ratios of < 1 at frequencies near 50 Hz. These data reveal that maximum acceleration levels of 2–7*g* are required in order to separate unencapsulated droplets at excitation frequencies from 5–50 Hz (Fig. 2c).

Bilayer formation and characterization in a high packing factor substrate

We form physically-encapsulated droplet interface bilayers in high-packing factor substrates that contains individual droplet compartments and integrated electrodes (Fig. 3a). The initial design of this substrate pairs the shape of the two-droplet well made by Funakoshi *et al.*[1] with the hemispherical divots machined by Holden *et al.*[2] The resulting substrate houses

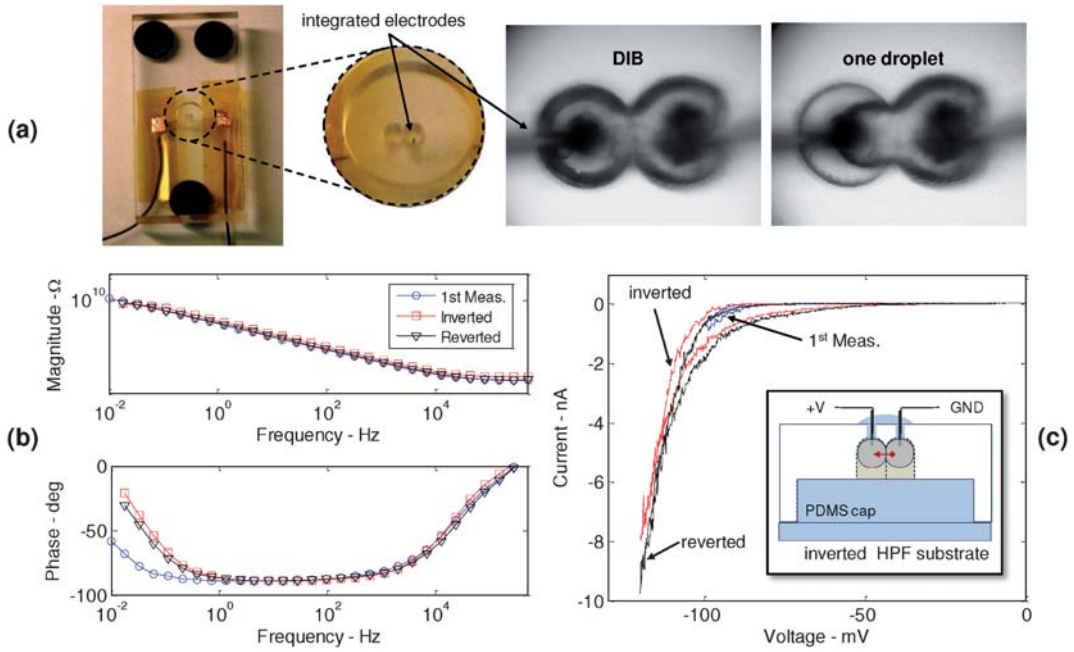

Fig. 3 Images of the high packing factor substrate show individual droplet compartments with integrated electrodes that extend vertically from the bottom of each well (a). An image of a DIB formed between two droplets within this substrate (left) is compared to the image of a ruptured bilayer that results in droplet coalescence (right). EIS (b) and CV (c) measurements for a physically-encapsulated DIB *via* the integrated electrodes display similar responses to those shown in Fig. 2 for unencapsulated DIBs. A PDMS plug is used to seal the droplets in their compartments after removing excess oil from the upper reservoir, permitting the entire substrate to be over-turned (inset shown in (c)).

a single droplet within each compartment where the overlapping compartments are positioned in order to promote bilayer formation between neighboring droplets. An upper reservoir in the fixture is designed for holding separated droplets in oil during monolayer formation. Custom Ag/AgCl electrodes built into the initial substrate provide access for interrogating specific interfaces within the network and simplify network assembly, where droplets are connected to one another and electrodes are inserted by merely "dragging and dropping" them into their respective compartments.

EIS data show that the low-frequency impedance of a droplet interface bilayer is typically higher than 1 GΩ and is often on the order of 100 GΩ (Fig. 3b). Fifteen different bilayers are formed between droplet pairs using the same high packing factor substrate in this study. Initial resistance values of the membranes prior to mechanical testing yields a distribution in which five bilayers had a resistance greater than 100 GΩ, five had nominal resistances between 1–100 GΩ, and five had resistances between 0.1–1 GΩ. The size of the interface varied from 80 μm in diameter to more than 340 μm in diameter (the average equivalent bilayer diameter was 267 ± 67 μm ($n = 15$)), even though a constant droplet volume of 350 nl is used in all trials. The initial specific membrane resistance (*resistance* × *area*) for physically-encapsulated DIBs formed in this study ranges from 0.1–100 MΩ cm^2, which compares well to previously published values for normalized bilayer resistance.[13,19,20]

The incorporation of voltage-sensitive alamethicin channels into physically-encapsulated droplet interface bilayers further confirms the formation of a lipid bilayer within the confined droplet compartments. Current–voltage traces presented in Fig. 3c show a marked change in the ability for ions to pass through the bilayer containing alamethicin channels *versus* the highly-resistive response of a pure lipid membrane (see Fig. 2b).[7] Specifically, an alamethicin-doped bilayer is highly-resistive in the "closed" state at applied potentials more positive than approximately −80 mV, but "turns on" at potentials more negative than −80 mV when aggregated alamethicin proteins form conductive pores through the bilayer that result in a large increase in the magnitude of current flowing through the membrane. Linear regressions applied to each of these regions shows that the bilayer containing alamethicin has an "off" resistance of approximately 17 GΩ that reduces by four orders of magnitude to a value of 1.9 MΩ in the "on" state. The rectification ratio for this membrane is approximately 10,000, much greater than a rectification of 60 measured for 10–15 genetically-modified alpha hemolysin (αHL) channels in DIBs.[6]

A distinct improvement over the liquid-in-liquid droplet interface bilayer platform is that physically-encapsulated DIBs can survive handling and even inversion of the entire substrate after bilayer formation. A press-fit, molded PDMS plug is used to seal the droplet networks in the lower droplet compartments of the substrate (shown in the inset in Fig. 3c) during inversion. Electrical measurements obtained *via* the integrated electrodes show that the interfacial lipid bilayer survives. The initial resistance of 38.4 GΩ, reduces to 5.5 GΩ after inversion and the size of the membrane also changes, reducing from an initial equivalent diameter of 430 μm to 326 μm. Both the resistance and diameter then increase to 7.5 GΩ and 390 μm, respectively, upon reversion to the initial orientation. These measurements suggest that the droplets "sag" vertically due to the higher density of the aqueous phase when the substrate is inverted. As a result, the bilayer unzips slightly but is retained since the droplets remain

anchored to the electrodes *via* the hydrophilic agarose coating. The voltage-dependent behavior of the proteins measured in both the upright and inverted orientations add additional proof that physical encapsulation protects the structure and functions of the system.

Quantifying the durability of encapsulated DIBs

Preliminary qualitative tests demonstrate that physical encapsulation of DIBs provides increased portability by limiting relative droplet movement. The geometry of the solid substrate confines the droplets to specific positions within the network that are maintained even when the solid substrate is manually handled, tilted, and inverted. The reduced volume of organic solvent surrounding the droplet, while only 10–100 μm thick, provides the necessary oil/water interface required for monolayer adsorption (which occurs on a length scale of 1–10 nm) and acts as a physical buffer between the liquid droplets and the solid exterior material.

The durability of droplet interface bilayers is quantified using a mechanical shaker to vibrate the droplets horizontally in a direction perpendicular to the bilayer interface. Impedance measurements using the integrated electrodes show that at low levels ($< \sim 0.5g$) of acceleration, shaking the DIBs results in a significant increase in the resistance of the bilayer. We attribute this increase in resistance to the incorporation of additional lipid molecules present within the aqueous droplet volume into the interfacial membrane and the continued self-ordering and packing of molecules residing in the fluid bilayer that occurs as the droplets are gently shaken. Representative measurements taken at three different frequencies on different DIBs show that this change in resistance is not necessarily accompanied by a change in the size of the bilayer as indicated by a nearly constant estimated interface diameter. Further, the measurements also show that at higher acceleration levels, the induced vibration reduces the resistance of the interface (again, a process independent of the bilayer size). This increase in bilayer resistance is observed consistently throughout the study, as shown in the histogram in Fig. 4c, though changes in bilayer size were significantly more varied. The size of the bilayer as estimated from capacitance values increased by an average of 100 μm in diameter from the initial measurement to the final measurement taken prior to bilayer failure, but with a large standard deviation of 220 μm.

The observed failure mode for encapsulated DIBs in the high packing factor substrate with electrodes is bilayer rupture, whereas similar tests performed on unencapsulated DIBs resulted in droplet separation. When fixed electrodes are not present, physically-encapsulated DIBs exhibit either separation or rupture. Failure consistently occurred between 1 and 10g of acceleration within the tested substrate geometries and frequency range. Droplet separation occurred several times in the high

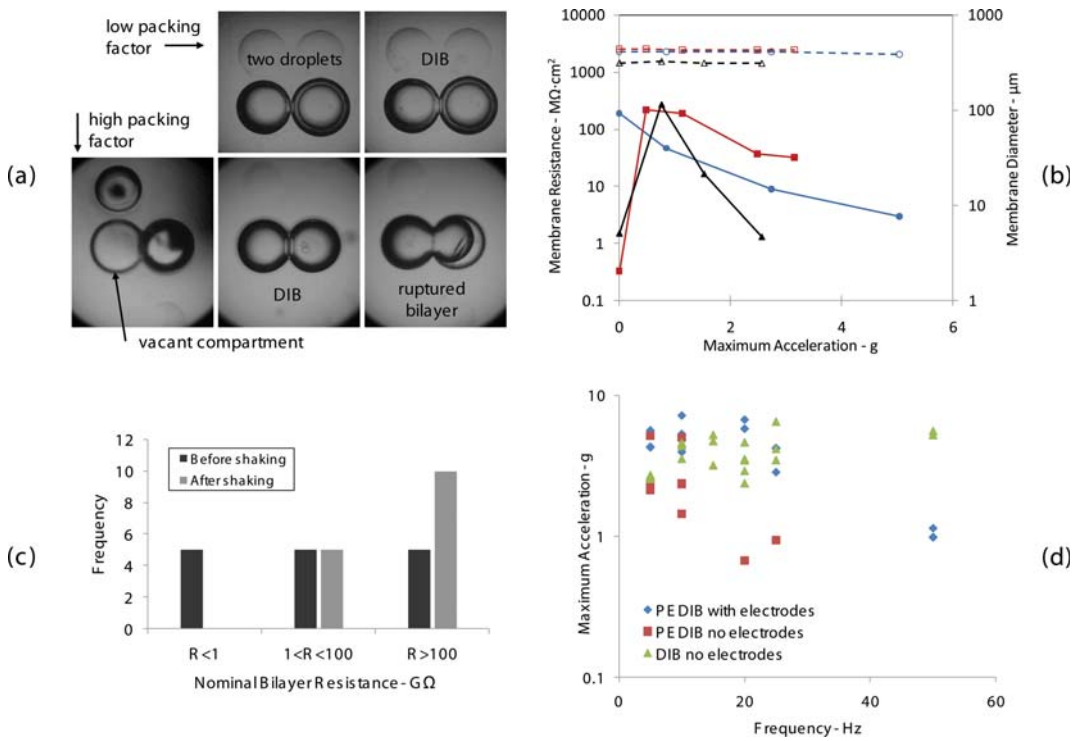

Fig. 4 The interfacial region between adjacent droplets lightens as the two monolayers zip together to form a bilayer, whereas the shadowed regions that trace the perimeters of the droplets result from the difference in refractive index at the oil/water interface (a). The membrane resistance (MΩ cm^2) and equivalent diameter (μm) extracted from EIS measurements of physically-encapsulated DIBs show that the resistance of the bilayer is affected differently at different levels of acceleration (b). A distribution of the initial (before shaking) values of nominal bilayer resistance *versus* the maximum values of measured nominal resistance after shaking for all fifteen trials (c). Measured values of maximum accelerations at failure for physically-encapsulated droplet interface bilayers (PEDIB) formed in similar high packing factor substrates with and without electrodes are compared to measured critical accelerations obtained for unencapsulated DIBs in the low packing factor substrate (d).

packing factor substrate when no electrodes were present. We observed that one of the droplets would move vertically into the upper reservoir, eventually separating from the other droplet. The presence of the integrated electrodes provides additional anchoring of the droplets and prevents separation. The data points show that physical encapsulation of droplet interface bilayers positioned on integrated electrodes does not greatly decrease the survivability of the bilayer. While physically-encapsulated droplet interface bilayers rupture at lower acceleration levels than those that cause separation of unencapsulated DIBs at frequencies higher than 20 Hz, they sustain larger accelerations than their unencapsulated counterparts at 5, 10, and 20 Hz. In comparison, Kang *et al* demonstrated that hydrogel-encapsulated bilayers were capable of surviving 5 min of shaking at 90 RPM (1.5 Hz), though no values of acceleration experienced by the substrate were reported.[21]

The different mode of bilayer failure is attributed to the small amount of organic solvent that encases the droplets. In a low packing factor substrate, the droplets experience minimal contact with the rigid PMMA substrate and separation is induced due to deformations of the droplets that unzip the interface. Physically-encapsulated droplets, however, undergo less relative motion and are buffered by a much smaller volume of organic solvent. The reduced amount of organic solvent surrounding physically-encapsulated DIBs absorbs less energy, allowing more to be transmitted directly to the droplets. We believe that this interaction also causes physically-encapsulated droplet interface bilayers to be less resistant to failure at higher frequencies (Fig. 4d). It is further suggested that with lower displacements and higher accelerations experienced at higher frequencies, the vibration begins to affect the molecules more than the droplets—whereupon the vibration essentially sonicates the system.

Physical encapsulation of multiple DIB networks

Physical encapsulation of DIBs within solid materials does not prohibit the formation of large biomolecular networks for lab-on-chip platforms. Instead, the methods presented herein establish a foundation on which larger, more-complex networks can be readily assembled given appropriate substrate design. A three-droplet network, featuring two droplet interface bilayers and integrated electrodes present in all compartments, is formed within a three-compartment substrate to demonstrate this principle. In the same manner that two-droplet networks were formed, three-droplet networks are assembled using the "drag and drop" technique for connecting droplets and inserting electrodes. The results presented in Fig. 5 show that the ability to tailor specific interfaces can still be achieved when the droplets are physically encapsulated. The upper-right droplet shown in Fig. 5a contains a mixture of lipid vesicles and alamethicin channels, while the other two droplets contain only the lipid vesicle solution. Impedance measurements performed across the interfaces individually and collectively ensure the formation of two lipid bilayers in the network (Fig. 5b). The resulting network displays different current–voltage behavior across each interface due to the incorporation of proteins into only one bilayer (Fig. 5c). The pure lipid membrane exhibits a typical resistive response in the CV measurement, while the second interface exhibits the voltage-dependent nature of a bilayer containing alamethicin channels.

Experimental

Substrate fabrication

Physically-encapsulated droplet interface bilayers are formed in a prototype high packing factor supporting substrate (Fig. 1b) made from an acrylic sheet (PMMA, McMaster-Carr). The initial concept pairs the shape of the simple two-droplet well made by Funakoshi *et al*[1] with the hemispherical divots machined by Holden *et al*.[2] The resulting substrate houses a single droplet within each compartment (1.02 mm in diameter and 1.5 mm deep) where the relative positioning of the overlapping compartments allows for intimate contact between neighboring droplets that leads to bilayer formation. An upper reservoir in the fixture is designed for holding separated droplets during monolayer formation. Custom silver–silver chloride (Ag/AgCl) electrodes built into the initial substrate are fabricated from 125 μm diameter silver wire (Goodfellow) that is chlorided in household bleach for one hour before being coated in 5% agarose gel (Sigma) in order to render the surface of the electrode hydrophilic.[2] The two electrodes are inserted through 300 μm diameter holes drilled through the substrate and held in place with a low-viscosity, light cure adhesive (Loctite 3104, Ellsworth Adhesives). The packing factor for 350 nl droplets within this

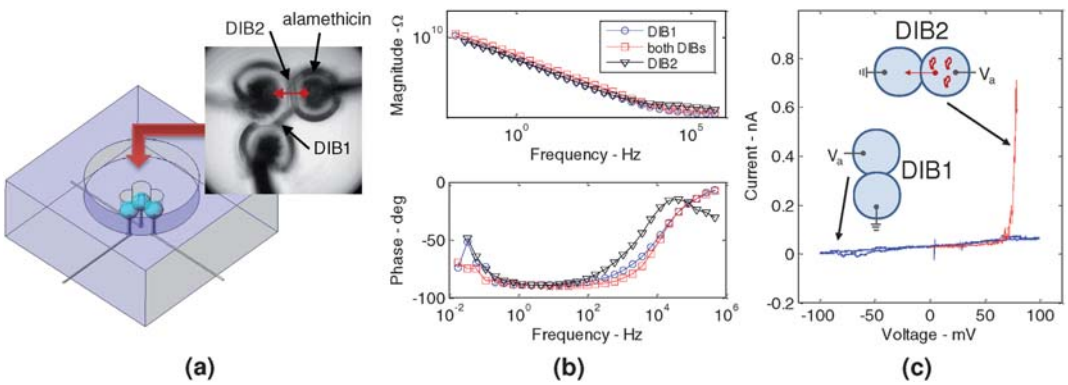

Fig. 5 A three-droplet network is formed that demonstrates the scalability of this technique for producing larger networks (a). The integrated electrodes provide access for investigating the electrical impedance (b) and current–voltage relationships (c) of each interface individually.

substrate exceeds 30%, when only the total volume of the droplet compartments is considered.

Materials

Aqueous droplets consist of a 2 mg/ml solution of 1, 2-diphytanoyl-*sn*-glycero-3-phosphocholine (DPhPC) phospholipid vesicles (purchased as lyophilized powder from Avanti Polar Lipids, Inc.) dissolved in 10 mM MOPS (Sigma), 100 mM NaCl (Sigma), pH 7 buffer solution and are submerged in hexadecane (Sigma) in order to form droplet interface bilayers. Phospholipid vesicles are prepared and stored as described elsewhere.[3] A period of 10–15 minutes after injection into hexadecane is given for monolayer stabilization before droplets are brought into contact. Alamethicin channels (A.G. Scientific) are stored in ethanol (Sigma) at 0.1% (w/v) and this stock solution is diluted further to a concentration of 100 μg/ml alamethicin in 10 mM MOPS, 100 mM NaCl, pH 7 buffer solution. Droplets containing alamethicin consist of a 50–2 (volume ratio) of vesicle solution–protein solution mixture that yields a final concentration of approximately 3.8 μg/ml of alamethicin within each droplet.

Droplet interface bilayer formation

Unencapsulated droplet interface bilayers are formed within a rectangular well (4 mm wide by 5 mm long by 3 mm deep) machined into a polymethyl-methacrylate (PMMA) acrylic substrate using previously established techniques.[2,7] A single DIB is formed between two droplets each approximately 350 nl in volume (~880 μm in diameter), producing a packing factor for this substrate and droplet size of 1.2%. Hemispherical divots machined into the bottom surface of this well provide discrete locations for the droplets to reside, but their shallow depths (0.25 mm) do not prevent droplet movement when the substrate is perturbed. A suspended Ag/AgCl electrode controlled by a 3-axis motorized micromanipulator (SM325, WPI Inc.) is used to position both droplets sequentially in these tests.

The formation of physically-encapsulated droplet interface bilayers must account for the immediate contact between neighboring droplets that occurs when the droplets are placed into adjacent compartments. Therefore, a single droplet is first injected into the hexadecane and moved into one of the droplet compartments where it is pierced by a fixed, wire-type Ag/AgCl electrode that extends vertically into the droplet compartment roughly 0.5 mm from the bottom surface of the well. Additional droplets are injected into the hexadecane and held in the upper reservoir to allow for monolayer formation to occur before network assembly. Droplets are moved into the remaining vacant droplet compartments in the lower region of the substrate after 15–20 minutes for monolayer formation. Electrode insertion again occurs as each droplet descends into its respective compartment. Bilayer formation between neighboring droplets occurs spontaneously within 2–3 minutes of initial contact.

Mechanical and electrical characterization

The durability of droplet interface bilayers is quantified using a Brüel and Kjaer 4810 mini-shaker to vibrate the droplets horizontally in a direction perpendicular to the bilayer interface. The shaker attaches directly to a platform on which the DIB substrates are mounted and is excited by a sinusoidal voltage waveform that is the output of a Siglab 20–42 data acquisition system and which is amplified using a Proton AA-1150 stereo power amplifier. The acceleration and displacement of the substrate are measured using an accelerometer (Piezotronics U352C22 and accompanying PCB Piezotronics 482A16 PZT charge coupler) and laser vibrometer (Polytec PDV-100), respectively. Durability tests are performed on the microscope stage of a Zeiss AxioVert 40CFL inverted microscope. Images and video are obtained through the objective lens of the microscope during and between tests using a Canon G6 digital camera and digital camera adapter.

Electrical impedance spectroscopy (EIS) and cyclic voltammetry (CV) are performed using an Autolab PGSTAT12 (Eco Chemie) Potentiostat/Galvanostat with a FRA2 module controlled by FRA and GPES software. Electrical impedance measurements of the DIBs are obtained using a 5 mV (RMS) sinusoidal potential swept from 500 kHz to 10 mHz. CV measurements are conducted with a scan rate of 2.5 mV/s and a step potential of 0.15 mV. A homemade Faraday cage surrounding the entire workstation is grounded through the Autolab device to an earth ground connection in order to minimize electrical noise during measurements.

Conclusion

Physical encapsulation of droplet interface bilayer networks transitions the original liquid-in-liquid DIB platform into a self-contained material system that will enable many lab-on-chip applications. A high packing factor substrate containing DIB networks can be moved, tilted, shaken, and even inverted while retaining the original molecular assembly and protein activity of the network. This approach overcomes the limited mobility of unencapsulated droplet networks and prevents droplet separation by reducing the volume of organic solvent that surrounds each droplet through substrate design. Integrated electrodes further simplify network formation and provide the necessary insertion into the aqueous phase for interrogating DIBs, all while retaining system mobility. The results of the mechanical testing both highlight (and quantify) the inherent durability of the droplet interface bilayers and suggest that substrate design can be used to minimize gross droplet movements which can limit the use of DIB networks in devices.

This work continues the development of the DIB method for creating new forms of active material systems that feature biomolecules organized in a manner similar to the cellular structures of natural tissues. Better methods for fabricating the exterior matrix are still required, and advances in the microfluidics field using naturally hydrophobic materials such as PDMS[22] will likely pave the way for designing sophisticated supporting structures with increased packing factor, generate femto- and pico-liter volume droplets,[23] and even route, sort, combine, and encapsulate (on the molecular scale) droplets within the outer matrix.[12,24,25] We believe that additional stability of the assembled networks may be gained by further reducing the size and impact of integrated silver–silver chloride electrodes *via* sharper profiles such as those developed by Kitade *et al.*[26] The development of dual-purpose, hollow electrodes also would enable the introduction of species into specific droplets into the

network after bilayer formation in addition to electrical interrogation. The number of uses for DIB platforms and other droplet-based technologies will likely continue to grow in number and complexity, and so further refinements in the techniques used to support, access, and interrogate biomolecular networks must keep pace.

References

1 K. Funakoshi, H. Suzuki and S. Takeuchi, *Anal. Chem.*, 2006, **78**, 8169–8174.
2 M. A. Holden, D. Needham and H. Bayley, *J. Am. Chem. Soc.*, 2007, **129**, 8650–8655.
3 W. L. Hwang, M. Chen, B. Cronin, M. A. Holden and H. Bayley, *J. Am. Chem. Soc.*, 2008, **130**, 5878–5879.
4 J. H. P. Bayley, M. Holden, A. J. Heron and D. Needham, *Formation of Bilayers of Amphiphatic Molecules*, 2008.
5 H. Bayley, B. Cronin, A. Heron, M. A. Holden, W. L. Hwang, R. Syeda, J. Thompson and M. Wallace, *Mol. BioSyst.*, 2008, **4**, 1191–1208.
6 G. Maglia, A. J. Heron, W. L. Hwang, M. A. Holden, E. Mikhailova, Q. Li, S. Cheley and H. Bayley, *Nat. Nanotechnol.*, 2009, **4**, 437–440.
7 S. A. Sarles and D. J. Leo, *J. Intell. Mater. Syst. Struct.*, 2009, **20**, 1233–1247.
8 D. D. Lasic and D. Needham, *Chem. Rev.*, 1995, **95**, 2601–2628.
9 A. Aharoni, G. Amitai, K. Bernath, S. Magdassi and D. S. Tawfik, *Chem. Biol.*, 2005, **12**, 1281–1289.
10 R. Syeda, M. A. Holden, W. L. Hwang and H. Bayley, *J. Am. Chem. Soc.*, 2008, **130**, 15543–15548.
11 D. S. Tawfik and A. D. Griffiths, *Nat. Biotechnol.*, 1998, **16**, 652–656.
12 S. Aghdaei, M. E. Sandison, M. Zagnoni, N. G. Green and H. Morgan, *Lab Chip*, 2008, **8**, 1617–1620.
13 W. Romer and C. Steinem, *Biophys. J.*, 2004, **86**, 955–965.
14 S. A. Sarles and D. J. Leo, *Encapsulated Bimolecular Networks*, 2009.
15 T. Baba, Y. Toshima, H. Minamikawa, M. Hato, K. Suzuki and N. Kamo, *Biochim. Biophys. Acta, Biomembr.*, 1999, **1421**, 91–102.
16 S. J. Archer and D. S. Cafiso, *Biophys. J.*, 1991, **60**, 380–388.
17 K. He, S. J. Ludtke, W. T. Heller and H. W. Huang, *Biophys. J.*, 1996, **71**, 2669–2679.
18 B. Bechinger, *J. Membr. Biol.*, 1997, **156**, 197–211.
19 P. Mueller, D. O. Rudin, H. T. Tien and W. C. Wescott, *Circulation*, 1962, **26**, 1167–1171.
20 P. Lauger, W. Lesslauer, E. Marti and J. Richter, *Biochim. Biophys. Acta*, 1967, **135**, 20–32.
21 X.-f. Kang, S. Cheley, A. C. Rice-Ficht and H. Bayley, *J. Am. Chem. Soc.*, 2007, **129**, 4701–4705.
22 L. Gitlin, P. Schulze and D. Belder, *Lab Chip*, 2009, **9**, 3000–3002.
23 R. M. Lorenz, J. S. Edgar, G. D. M. Jeffries and D. T. Chiu, *Anal. Chem.*, 2006, **78**, 6433–6439.
24 M. He, J. S. Edgar, G. D. M. Jeffries, R. M. Lorenz, J. P. Shelby and D. T. Chiu, *Anal. Chem.*, 2005, **77**, 1539–1544.
25 S.-Y. Teh, R. Lin, L.-H. Hung and A. P. Lee, *Lab Chip*, 2008, **8**, 198–220.
26 T. Kitade, K. Kitamura, S. Takegami, Y. Miyata, M. Nagatomo, T. Sakaguchi and M. Furukawa, *Anal. Sci.*, 2005, **21**, 907–912.